Journal of the Optical Society of Korea
Vol. 20, No. 4, August 2016, pp. 524-529

ISSN: 1226-4776(Print) / ISSN: 2093-6885(Online)
DOI: http://dx.doi.org/10.3807/JOSK.2016.20.4.524

In-Line Hologram for Plasma Diagnostics

Byungwhan Kim* and Jin-Su Jung

Department of Electrical Engineering, Sejong University, Seoul 05006, Korea

(Received December 17, 2015 : revised May 12, 2016 : accepted June 17, 2016)

Diagnostic sensors are demanded during plasma processes. Holograms of plasma taken with laser light without a reference beam were used to monitor behaviors of charged particles produced in nitrogen plasma as a function of electrode temperature ranging between 50 and 300℃. Holograms were characterized as a function of the pixel sum and grayscale value. Pixel sum calculated in identified grayscale ranges strongly correlated with ion density and emitted light intensity measured with a langmuir probe and optical emission spectroscopy, respectively. The performance was further evaluated with data acquired as a function of N_2 and NH_3 flow rates and improved correlations were observed in the new grayscale range. The confirmed correlations indicate that a hologram is a viable means to diagnose behaviors of plasma particles such as ions. Underlying principles are discussed in view of particle and charge composing vacuum and light.

Keywords : Plasma, Vacuum, Laser, Light, Hologram
OCIS codes : (280.0280) Remote sensing and sensors; (120.6150) Speckle imaging; (120.1880) Detection

I. INTRODUCTION

Plasma plays a crucial role in depositing and etching nano-scaled thin films employed in fabricating electronic devices. Of various plasma sensors, optical emission spectroscopy (OES) and the langmuir probe are the most widely adopted for plasma monitoring. The OES provides optical data such as the light intensity emitted from the plasma. In contrast, the langmuir probe offers electrical data such as the electron density and electron temperature.

For plasma diagnostics, laser has been used to generate a plasma called "laser-induced plasma (LIP)" [1-4]. A spectral line profile [1] or self absorption phenomenon [2] occurring in the LIP was used to determine the electron number density for plasma diagnostics. The temperature of the LIP was characterized using infrared spectral lines [3]. The interaction of laser pulse with matter particle was investigated with X-ray diagnostics [4]. Another diagnostic method referred to as the digital in-line holography (DIH) differs from the LIP in that laser directly interacts with the micron-sized particles termed "dust" in three-dimensional (3-D) plasma space. The DIH has been used to study 3-D dust behaviors [5, 6]. It is based on the recording of diffraction patterns formed by the two reference and object beams. Despite promising results in the dusty plasmas, the DIH was unable to provide details on plasma matter particles such as the ions or electrons. To overcome this limitation, a variant of the DIH was introduced [7, 8] and it fundamentally differs from the existing DIH because it relies only upon the object beam. In other words, the DIH variant does not require the formation of diffraction patterns. Rather, it records interaction between laser light and plasma particles.

The applications of the DIH variant [7, 8] demonstrated that diagnostic variables extracted from the holograms recorded on a charge-coupled device (CCD) sensor well correlated to the emitted light intensity [7, 8] or ion density [8]. This signifies that the hologram is capable of containing information on the variation of ions or light of plasma. From this perspective, the hologram obtained without the reference beam is a kind of an in-line hologram, very close to the one utilized in earlier work [9]. Despite promising features of the DIH variant, its performance has not been fully evaluated under a wide range of plasma. The reported correlations [8], especially with the ion density, need further improvement. Moreover, it is still challenging to analyze speckle-like holograms for the identification of individual matter particles such as ions

*Corresponding author: kbwhan@sejong.ac.kr

Color versions of one or more of the figures in this paper are available online.

or electrons. Most of all, more studies in both theoretical and experimental ways are in demand to understand underlying principles of the DIH variant. A qualitative model proposed in the work [8] is one of the efforts.

In this work, we present other experimental data evaluated in N_2 plasma as a function of the electrode temperature. As carried out in the works [7, 8], a pixel sum distribution function (PSDF) was derived from each hologram. Diagnostic variables such as the pixel sum are compared to others offered from the typical plasma sensors such as OES and langmuir probe. This work reports on the ranges of grayscale values considerably improving the correlation. This is further evaluated with other data collected with the variation of two gas flow rates already examined in [8]. The mechanism once proposed for the explanation of the correlations [8] is supported by evidence on vacuum properties inferred from a hologram of vacuum.

II. METHODS

The schematic of the hologram imaging system was once reported [7, 8]. It was composed of a Nd:Yag laser operating at a wavelength of 532 nm, a beam expander, and a charge-coupled device sensor. Plasma was created in N_2 plasma as a function of the electrode temperature, varied from 50 to 300℃ using a temperature controller. The rf source and bias powers were set to 300 and 0 W, respectively. The pressure of a vacuum chamber was not controlled. Under the same plasma conditions, emitted light intensity and ion density along with the electron were acquired with OES and Langmuir probe, respectively. The probe tip was placed near the center of a plasma body generated in a cylindrical shaped chamber 17 cm high and 25 cm in diameter. The tip position was about 7 cm under the top surface of the chamber and two glass windows were placed at the front and rear of the chamber for light to pass.

III. RESULTS

3.1. Characterization of Pixel Sum Distribution Function

As an illustration, Fig. 1 shows a hologram of plasma created at 50℃. The other holograms taken at other temperatures were very similar to this one. The hologram looks relatively dark and the lower darker region represents the electrode. Information concealed in the hologram of Fig. 1 is characterized in terms of the grayscale and pixel sum as carried out in the earlier works [7, 8]. The resulting distribution is termed the "pixel sum distribution function (PSDF)". The PSDFs extracted from the holograms are shown in Fig. 2. In obtaining the PSDFs, original holograms were used rather than the resolution-adjusted ones such as the one of Fig. 1. Here, the pixel sum is calculated as the sum of the pixels with the same grayscale. As illustrated in Fig.

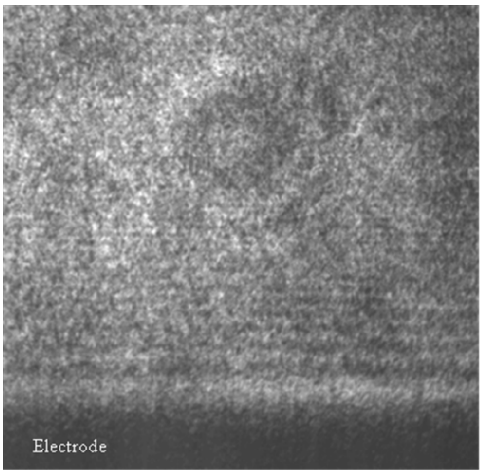

FIG. 1. Laser hologram of plasma created at 50℃. The brightness and contrast of the original hologram was adjusted to 28 and 73 respectively using the Photoshop.

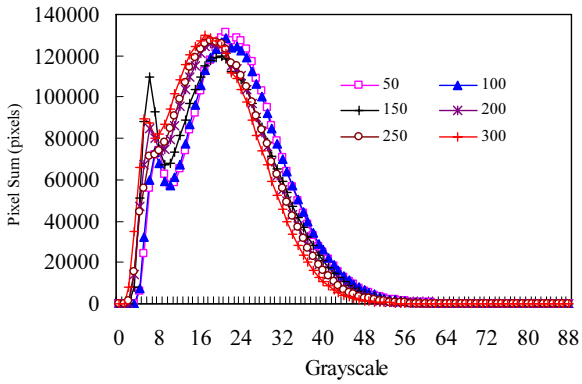

FIG. 2. PSDFs characterized as a function of the temperature.

2, each PSDF is comprised of the two sub-PSDFs peaking at different grayscales. It was known that the grayscale range between 0 and the one at which the first peak of the first sub-PSDF occurs represents the electrode. As this grayscale range is excluded, the overall grayscale range of concern is restricted to between the first peak and the end of the second sub-PSDF.

Apart from the peaks, a transition is observed at the same 21 grayscale irrespective of the temperature levels. This can be confirmed from Fig. 3 and the transition at 300℃ is more evident. With respect to the specific grayscale values matching the peak or the transition, several grayscale ranges may be considered for plasma diagnostics. It was observed that the grayscale ranges initiating from either the second peak or the transition correlated little with the data measured with the plasma sensors to be presented later. The grayscale ranges are restricted to the three ones. The first grayscale range is between the first peak and transition. The first peaks occur at 8, 7, 6, 6, 6, and 5 at 50, 100, 150, 200, 250, and 300℃, respectively. The second one is between the ending grayscale of the first sub-PSDF and the transition.

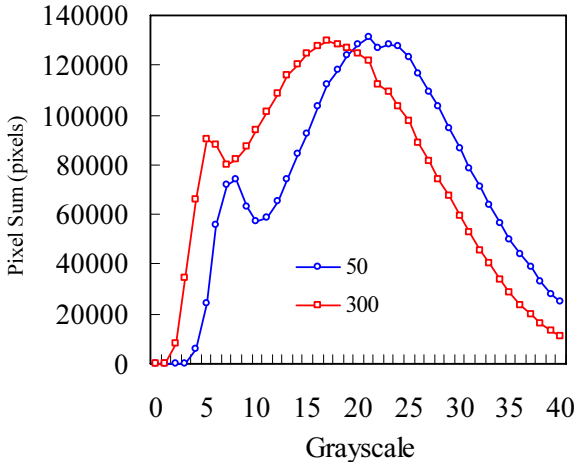

FIG. 3. Comparison of two PSDFs of plasma taken at 50 and 300℃.

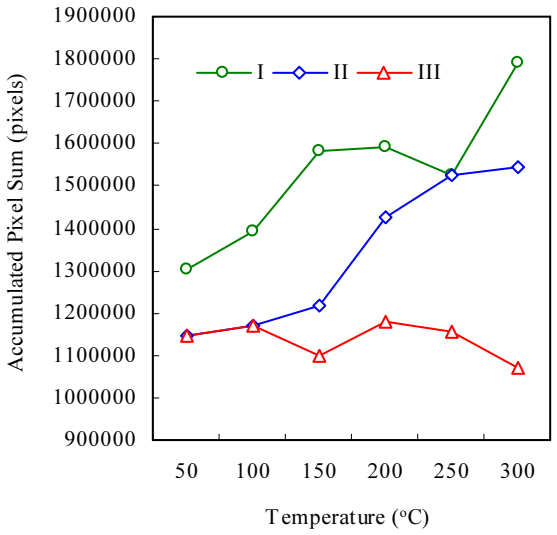

FIG. 4. Variation of pixel sums with the temperature in three grayscale ranges.

The ending grayscales of first sub-PSDFs occur at 10, 10, 9, 8, 6 and 8 at 50, 100, 150, 200, 250, and 300℃, respectively. The third one is between the ending grayscales stated earlier and second peak. The second peaks occur at 21, 21, 20, 19, 18, and 18 at 50, 100, 150, 200, 250, and 300℃, respectively. The three types of grayscale ranges mentioned are referred to as types I, II, and III. In order to monitor variations of pixel sums with the type, an accumulated pixel sum (APS) is defined as the sum of all individual pixel sums calculated over all the grayscale values belonging to each type. The calculated APSs for the 3 types are shown in Fig. 4.

3.2. Comparisons with In-situ Plasma Sensors

For comparison purpose, ion density was measured with the langmuir probe. As illustrated in Fig. 5, the ion density

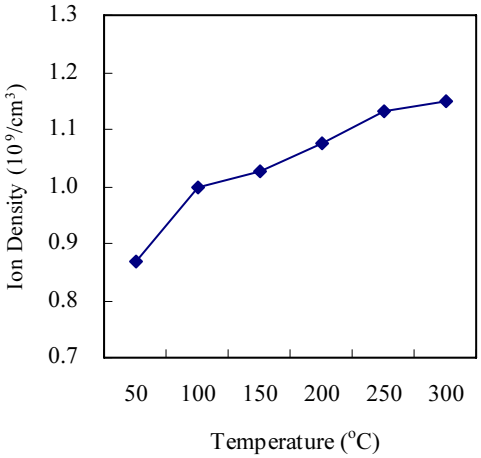

FIG. 5. Variation of ion density with the temperature.

continues to increase with increasing the temperature due to the enhanced ionization of atoms at higher temperatures. As compared to Fig. 4, Fig. 5 reveals that the ion density variation is very close to the one of the type II in Fig. 4. This indicates that the respective APS can represent the variations of ion density. The grayscale values involved in the type II then represent energy states of particles (mostly electrons) comprising the ions.

Possible correlation with the emitted light intensity is more evaluated with the data obtained with OES. The OES spectra acquired are shown in Fig 6 as a function of the temperature. The variations of peak intensities with the temperature are plotted in Fig. 7. All the peak intensities except for one deviation at the longest wavelength of 772.967 nm incline to increase with increasing the temperature. The increasing tendency is very similar to that of the type II of Fig. 4. The emitted light variation at 380.519 nm is nearly identical to that of the type II. Similar coincidence was observed in the N_2 plasmas [7, 8]. Therefore, it is known that the hologram can also provide information on the emitted light intensity as well as the ion density.

The performance of the method at the identified grayscale range is further evaluated with the plasma data generated in N_2 and NH_3 gases. The holograms and PSDFs of these data were already presented [8]. In earlier work [8], relatively large differences were noted between the pixel sum (here the APS) and ion density variations despite the similarity in the overall tendency. The differences were more pronounced in the NH_3 plasma. It must be noted that the smallest and largest grayscale values composing the grayscale range employed in that study corresponded to the first peak and middle of the first and second peaks. For convenience, the grayscale range identified in this study is denoted as the "current range". The current range in the N_2 plasma is the same as 51-85 for all PSDFs. However, it is different in the NH_3 plasma because the ending grayscale of the first sub-PSDF is different depending on the flow rate. In contrast, the transition occurred at the same 72. The grayscale ranges

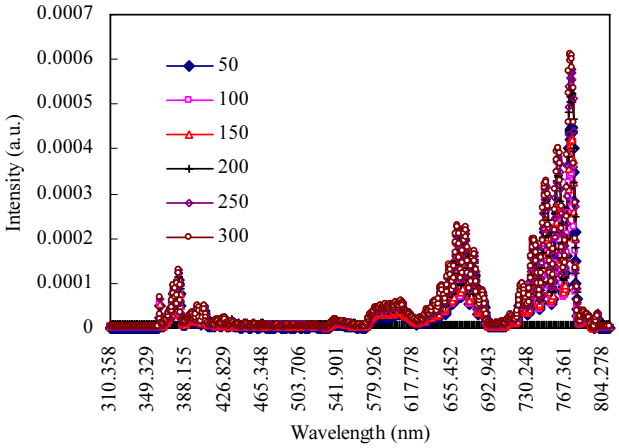

FIG. 6. Spectra of emitted light intensity measured with optical emission spectroscopy.

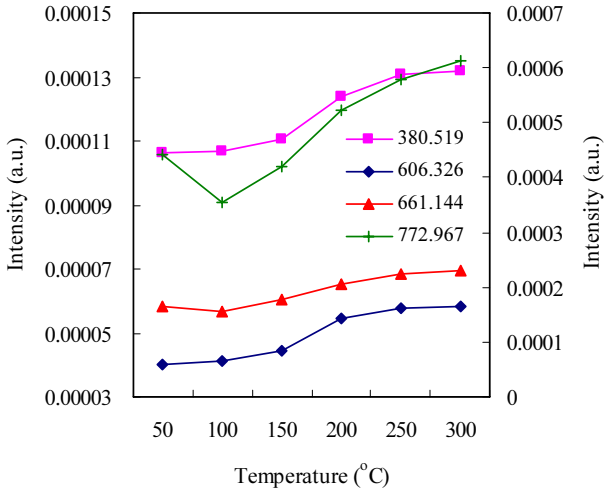

FIG. 7. Variation of light intensity as a function of the temperature.

are then chosen as 35-72, 32-72, 30-72, 31-72, 30-72, and 28-72 at 3, 6, 9, 12, 15, and 18 sccm, respectively. Meanwhile, we evaluated the performance in another grayscale range called "new range", defined between the smallest grayscale value of "0" and the ending grayscale one mentioned earlier. In the N_2 plasma, it is "0-51" in all the PSDFs. In the NH_3 plasma, it becomes 0-35, 0-32, 0-30, 0-31, 0-30, and 0-28 at 3, 6, 9, 12, 15, and 18 sccm, respectively.

Figure 8 shows comparisons of the APSs calculated in the two grayscale ranges. In previous work [8], the ion density continued to decrease with the N_2 flow rate. As compared to this variation, the APS calculated in the current range shows some deviations in the flow rate range of 15-18 sccm as the previous one [8]. By contrast, the APS tendency calculated in the new range is in good agreement over the entire flow rate. The APS variation with the NH_3 flow rate is shown in Fig. 9. The work [8] showed that the ion density

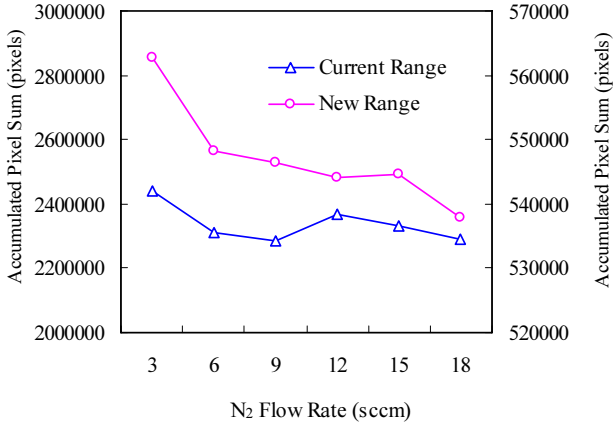

FIG. 8. Variation of accumulated pixel sums with the N_2 flow rate.

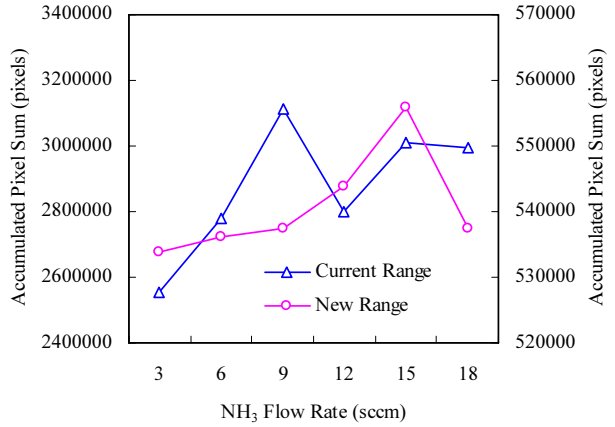

FIG. 9. Variation of accumulated pixel sums with the NH_3 flow rate.

continued to increase until 15 sccm and then decreased at 18 sccm. The APS calculated in the current range does not match the reported ion density variation in the flow rate range of 12-18 sccm. However, the APS computed in the new range coincides well with the ion density variation. Noticeably, this correlation is much improved as compared to the reported one [8]. Therefore, it is demonstrated that the new range is more effective in characterizing ion density behavior with the gas flow rate.

IV. DISCUSSION

The correlations confirmed in this study indicate that the holograms certainly contain information on the behaviors of plasma ions or light. This is only possible as an electromagnetic field is formed along the path of the light beam as stated in the proposed model [8]. According to the model, the field is established by the vacuum presumed to be negative in charge and light inferred to have positive charge [10]. As the generated plasma particles interact

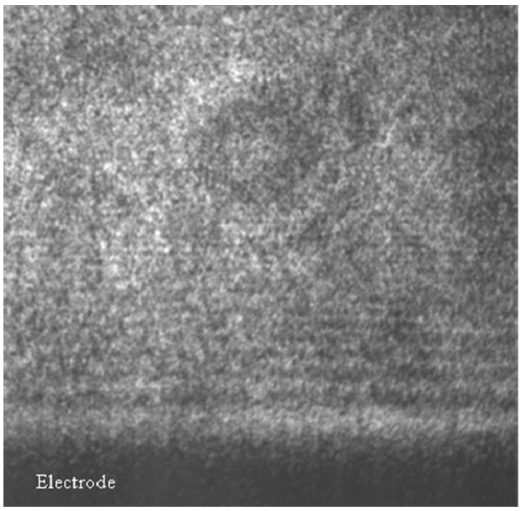

FIG. 10. Laser hologram of vacuum space at 50℃. The brightness and contrast of the original hologram was adjusted to 28 and 73 respectively using the Photoshop.

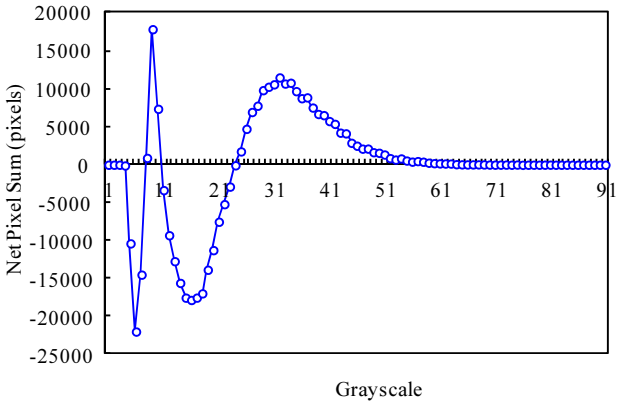

FIG. 11. Variation of net pixel sums as a function of the temperature.

with the field, the PSDF changes and quantifying them in terms of the pixel sum or APS is the core of the hologram analysis.

Then, the next concern is how the electromagnetic field is generated. To explore this, another hologram of vacuum was taken at the temperature same as the one of Fig. 1. It is noticeable that the vacuum hologram of Fig. 10 is very similar to the plasma one of Fig. 1. The differences between them can be quantified by subtracting the PSDF of vacuum hologram from that of plasma. The resulting Fig. 11 shows that positive pixel sums occur in the two grayscale ranges of 10-12 and 24-77. The particles belonging to them become the net ones sorely attributable to the plasma. This illustration signifies that the net variation of plasma particles could be quantified using the PSDF of vacuum as a reference one [11]. Meanwhile, the identified two grayscales are part of the existing PSDFs. This supports that plasma particles pass through the hologram space prepared by the laser light.

Certainly, the holograms are generated by the laser light. As reported, the light is composed of hard matter and transparent particles [12]. This means that this light alone is unable to form such speckle-like dark holograms as shown in Fig. 1 and Fig. 10. In other words, those dark matter particles included in them are not associated with light. Instead, they are likely to belong to the vacuum. The existence of dark particles in the vacuum is supported by the two holograms both in vacuum and plasma.

The vacuum is regarded to have a zero-point energy and has certain fluctuations as confirmed from the Casimir effect [13] or their visualization [14]. In the context of vacuum particles, it was experimentally observed that injecting laser light into the vacuum led to the generation of electron-positron pairs (EPPs) [15]. The generation of the EPPs has been interpreted as the process of excitations of quasi vacuum particles in an external field. The quasiparticles are presumed to have the quantum numbers of the positron and electron and change into EPPs in the quantum way as the excitation ceases. Without relying upon the quantum transition, the occurrence of EPPs can be interpreted differently with reference to the reported positive light [10]. The report [10] stated that light is composed of positive particles such as the positron. As this argument is applied, the electron of the EPPs belongs to the vacuum particle. This suggested negative electron in the vacuum is consistent with the proposed vacuum model of “sea of electrons” [16].

Basing on the presumed negative particles filling the vacuum, the EPP generation might be explained as follows: an injection of positive light containing positrons, transfer of the positive charge of the positrons to the negative electrons, and creation of EPPs. The EPPs are unable to be created as either the electron in the vacuum or the positron of light is not present in the vacuum. The suggested process indicates that the EPP occurrence is not a quantum process, but a well expected process given the negative vacuum and positive light particles as once mentioned in the plasma [8]. The validity of the negative vacuum is more supported by the recent theoretical result, arguing that the vacuum is negative [17]. Meanwhile, it is not certain how the negative vacuum particles are engaged in the generation of the plasma. This demands clarification of interaction among the vacuum particles, externally supplied field, and atoms fed into a vacuum chamber. In the recent report, it was argued in proposing a new light emission process from an atom that the vacuum particles serve as a medium of transferring external energy to the atoms [18].

V. CONCLUSION

This work demonstrated that plasma particles could be monitored using the holograms taken with the laser employing only the object beam. The confirmed strong correlations with the typical plasma sensor data demonstrated that the

holograms could contain information on particle behaviors characterized by the PSDF. The application of the PSDF is well able to be extended for the identification of other particles such as the electrons or positrons besides the ion density or light as investigated in this work. Counting matter particles of plasma is not possible without the formation of electromagnetic field in the vacuum, enabled by the positive light and negative vacuum. The hologram of vacuum and reported light properties played a crucial role in identifying dark particles of vacuum and understanding their interaction with the positive light. This led to the proposition of a new mechanism for the EPP generation. In the context of analysis of holograms, more study is needed for the identification of relevant grayscale ranges depending on the plasma particles under various plasma conditions.

ACKNOWLEDGMENT

This research was supported by Basic Science Research Program through the National Research Foundation of Korea (NRF) funded by the Ministry of Education, Science and Technology (2012R1A1A2008720).

REFERENCES

1. M. Cvejić, M. R. Gavrilović, S. Jovićević, S, E. Stambulchik, and N. Konjević, "Neutral lithium spectral line 460.28 nm with forbidden component for low temperature plasma diagnostics of laser-induced plasma," Spectrochim. Acta B **100**, 86-97 (2014).
2. M. Cvejić, M. R. Gavrilović, S. Jovićević, and N. Konjević, "Stark broadening of Mg I and Mg II spectral lines and Debye shielding effect in laser induced plasma," Spectrochim. Acta Part B **85**, 20-33 (2013).
3. J. He, Q. Zhang, and L. Liao, "Temperature diagnostic for laser-induced plasma by electron collision model," Mod. Phys. Lett. B **29**, 1550138 (2015).
4. I. Yu. Skobelev, A. Ya. Faenov, S. V. Gasilov, T. A. Pikuz, A. I. Magunov, A. S. Boldarev, and V. A. Gasilov, "Diagnostics of plasma produced by femtosecond laser pulse impact upon a target with an internal nanostructure," Plasma Phys. Rep. **36**, 1261-1268 (2010).
5. M. Kroll, S. Harms, D. Block, and A. Piel, "Digital in-line holography of dusty plasmas," Phys. Plasmas **15**, 063703 (2008).
6. F. Corinne, D. Christophe, and F. Thierry, "Digital in-line holography: influence of the reconstruction function on the axial profile of a reconstructed particle image," Meas. Sci. Technol. **15**, 686-693 (2004).
7. B. Kim, D. Jung, and D. Han, "Plasma sensor for monitoring laser-interacting particles in contact with an electrode," Electron. Mat. Lett. **10**, 655-659 (2014).
8. B. Kim, D. Jung, J. Seo, J. Lee, and J. Seo, "Monitoring of nitrogen plasma using laser hologram, J. Nanoelectron. Optoe. **11**, 103-107 (2016).
9. M. Centurion, Y. Pu, Z. Liu, and D. Psaltis, "Holographic recording of laser-induced plasma," Opt. Lett. **29**, 772-773 (2004).
10. B. Kim, "Positive light matter," IJLRST **4**, 4-6 (2015).
11. B. Kim, "Monitoring system of vacuum and plasma and method thereof," Patent, KR1305049 (2013).
12. B. Kim, "Collection of photons," IJLRST **3**, 1-11 (2014).
13. H. B. G. Casimir, "On the attraction between two perfectly conducting plates," Proc. K. Ned. Akad. Wet. B **51**, 793-795 (1948).
14. M. Lee, J. Kim, W. Seo, H. G. Hong, Y. Song, R. R. Dasari, and K. An, "Three-dimensional imaging of cavity vacuum with single atoms localized by a nanohole array," Nat. Commun. **5**, 3441 (2014).
15. D. B. Blaschke, B. Kaempfer, S. M. Schmidt, A. D. Panferov, A. V. Prozorkevich, and S. A. Smolyansky, "Properties of the electron-positron plasma created from vacuum in a strong laser field. Quasiparticle excitations," Phys. Rev. D **88**, 045017 (2013).
16. P. A. M. Dirac, "The quantum theory of the electron," Proc. R. Soc. Lond. A **117**, 610-624 (1928).
17. A. Hickling and T. Wiseman, "Vacuum energy is non-positive for (2+1)-dimensional holographic CFTs," Class. Quant. Grav. **33**, 044001-0455009 (2016).
18. B. Kim, "New process of light emission in plasma," in *Proc. 2016 Spring Conference of Korean Physical Society* (Daejeon Convention Center, Daejeon, Korea, April 20-22, 2016), p. 38.